International Research Journal of Engineering and Technology (IRJET) e-ISSN: 2395-0056
Volume: 02 Issue: 07 | Oct-2015 www.irjet.net p-ISSN: 2395-0072

A SUPER CAPACITOR BASED POWER CONDITIONING SYSTEM FOR POWER QUALITY IMPROVEMENT

Sujith R. Injeti, K. Padma

Andhra University , Visakhapatnam

Andhra Pradesh, India.

Abstract: *Introducing of various types of distributed energy resources (DERs) like solar and wind onto the distribution grid is a trend. Due to this there is a corresponding increase in power quality problems and power irregularities on the distribution grid. In order to reduce the irregularities and improve the power quality of the distribution grid, an super capacitor integrated power conditioner is proposed in this paper. Super capacitor integration gives the power conditioner active power capability, which is useful in tackling the grid output irregularities and in improving the voltage sag and swell compensation. Super capacitors have low energy density, high-power density, and fast charge/discharge rates, which are all ideal characteristics for meeting high-power low-energy events like grid intermittencies, sags/swells. In this paper, super capacitor is integrated into dc-link of the power conditioner through a bidirectional dc–dc converter that helps in providing a stiff dc-link voltage. The integration helps in providing active/reactive power support, intermittency smoothing, and sag/swell compensation. Design and control of both the dc–ac inverters and the dc–dc converter are discussed. The simulation model of the overall system is developed.*

INTRODUCTION

Power quality is major cause of concern in the industry, and it is important to maintain good power quality on the grid. Therefore, there is renewed interest in power quality products like the active power filter (APF) and dynamic voltage restorer (DVR). APF prevents the grid from supplying non-sinusoidal currents when the load is nonlinear [3] and DVR prevents sensitive loads from experiencing voltage sags/swells [1], [2]. The concept of integrating the APF and DVR through a back–back inverter topology was first introduced in [4] and the topology was named as unified power quality conditioner (UPQC). The design goal of the traditional UPQC was limited to improve the power quality of the distribution grid by being able to provide sag, swell, and harmonic current compensation. In this paper, energy storage integration into the power conditioner topology is being proposed, which will allow the integrated system to provide additional functionality. With the increase in penetration of the distribution energy resources (DERs) there is a corresponding increase in the power quality problems and intermittencies on the distribution grid in the *seconds* to *minutes* time scale [5]. Energy storage integration with DERs is a potential solution, which will increase the reliability of the DERs by reducing the intermittencies and also aid in tackling some of the power quality problems on the distribution grid [5]–[8]. Applications where energy storage integration will improve the functionality are being identified, and efforts are being made to make energy storage integration commercially viable on a large scale [9], [10]. Smoothing of DERs is one application where energy storage integration and optimal control play an important role [11]–[17]. In [11], super capacitor and flow battery hybrid energy storage system are integrated into the wind turbine generator to provide wind power smoothing, and the system is tested using a real-time simulator. In [12], super capacitor is used as an auxiliary energy storage for photovoltaic (PV)/fuel cell, and a model-based controller is developed for providing optimal control. In [13], a battery energy storage system-based control to mitigate wind/PV fluctuations is proposed. In [14], multiobjective optimization method to integrate battery storage for improving PV integration into the distribution grid is proposed. In [15], a theoretical analysis is performed to determine the upper and lower bounds of the battery size for grid-connected PV systems. In [16], a rule-based control is proposed to optimize the battery discharge while dispatching intermittent renewable resources. In [17], optimal sizing of a zinc bromine-based energy storage system for reducing the intermittencies in wind power is proposed. It is clear from the literature that renewable intermittency smoothing is one application that requires active power support from energy storage in the *seconds* to *minutes* time scale

[10]. Reactive power support is another application which is gaining wide recognition with proposals for reactive power pricing. Voltage sag and swells are power quality problems on distribution grid that have to be mitigated. Sag/swell compensation needs active power support from the energy storage in the *milliseconds* to *1 min* duration [11]. All the above functionalities can be realized by integrating energy storage into the grid through a power conditioner topology. Of all the rechargeable energy storage technologies super- conducting magnet energy storage (SMES), flywheel energy storage system (FESS), battery energy storage system (BESS), and ultracapacitors (UCAPs), UCAPs are ideal for providing active power support for events on the distribution grid which require active power support in the *seconds* to *minutes* time scale like voltage sags/swells, active/reactive power support, and renewable intermittency smoothing [7]. In this paper, UCAP-based energy storage integration through a power conditioner into the distribution grid is proposed, and the following application areas are addressed.

1) Integration of the super capacitor or UCAP with power conditioner system gives the system *active power capability.*
2) Experimental validation of the super capacitor or UCAP, dc–dc converter, inverter their interface, and control.
3) Development of inverter and dc–dc converter controls to provide sag/swell compensation and active/reactive support to the distribution grid.

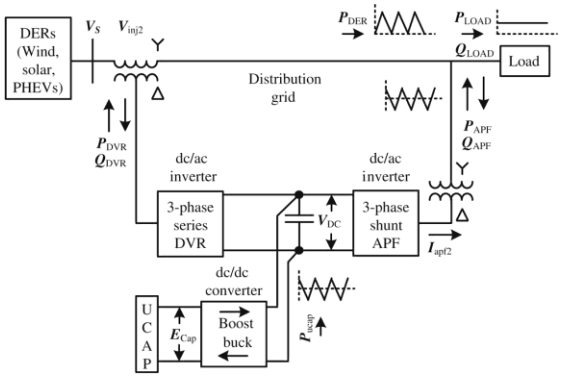

Fig. 1. One-line diagram of power conditioner with UCAP energy storage.

II. THREE-PHASEINVERTERS

A.Power Stage

The one-line diagram of the system is shown in Fig.1. The power stage consists of two back-to-back three-phase voltage source inverters connected through a

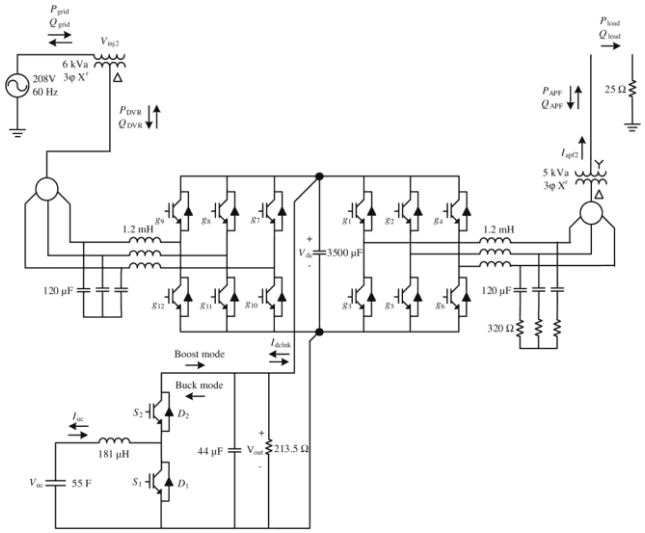

dc- link capacitor. UCAP energy storage is connected to the dc-link capacitor through a bidirectional dc–dc

Fig. 2. Model of power conditioner with UCAP energy storage.

converter. The series inverter is responsible for compensating the voltage sags and swells; and the shunt inverter is responsible for active/reactive power support and renewable intermittency smoothing. The complete circuit diagram of the series DVR, shunt APF, and the bidirectional dc–dc converter is shown in Fig.2. Both the inverter systems consist of IGBT module, its gate driver, LC filter, and an isolation transformer. The dc-link voltage Vdc is regulated at 260V for optimum voltage and current compensation of the converter and the line–line voltage Vab is 208V. The goal of this project is to provide the integrated power conditioner and UCAP system with active power capability 1) to compensate temporary voltage sag (0.1–0.9p.u.) and swell (1.1–1.2p.u.), which last from 3s to 1min[18]; and 2)to provide active/reactive support and renewable intermittency smoothing, which is in the seconds to minutes time scale.

B. Controller Implementation

The series inverter controller implementation is based on the *in-phase compensation* method that requires PLL for estimating θ, and this has been implemented using the *fictitious power method* described in [4]. Based on the estimated θ and the line–line source, voltages *Vab*, *Vbc*, *Vca* (which are available for this delta-sourced system) are transformed into the d–q domain and the line–

neutral components of the source voltage V_{Sa}, V_{Sb}, and V_{SC} which are not available can then be estimated using.

$$\begin{bmatrix} V_{sa} \\ V_{sb} \\ V_{sc} \end{bmatrix} = \begin{bmatrix} 1 & 0 \\ -\frac{1}{2} & \frac{\sqrt{3}}{2} \\ -\frac{1}{2} & -\frac{\sqrt{3}}{2} \end{bmatrix} \begin{bmatrix} \cos(\theta - \frac{\pi}{6}) & \sin(\theta - \frac{\pi}{6}) \\ -\sin(\theta - \frac{\pi}{6}) & \cos(\theta - \frac{\pi}{6}) \end{bmatrix} \begin{bmatrix} \frac{V_d}{\sqrt{2}} \\ \frac{V_q}{\sqrt{2}} \end{bmatrix} \quad (1)$$

$$\begin{bmatrix} V_{refa} \\ V_{refb} \\ V_{refc} \end{bmatrix} = m^* \begin{bmatrix} (\sin\theta - \frac{V_{sa}}{169.7}) \\ (\sin\theta - \frac{2\pi}{3} - \frac{V_{sb}}{169.7}) \\ (\sin\theta + \frac{2\pi}{3} - \frac{V_{sc}}{169.7}) \end{bmatrix} \quad (2)$$

$$P_{dvr} = 3V_{inj2a(rms)}\ 3I_{La(rms)} cos\varphi \quad (3)$$
$$Q_{dvr} = 3V_{inj2a(rms)}\ 3I_{La(rms)} sin\varphi$$

These voltages are normalized to unit sine waves using line–neutral system voltage of 120 Vrms as reference and compared with unit sine waves *in-phase* with actual system voltages V_S from (2) to find the injected voltage references Vref necessary to maintain a constant voltage at the load terminals, where m is the modulation index, which is 0.45 for this case. Therefore, whenever there is a voltage sag or swell on the source side, a corresponding voltage Vinj2 is injected in-phase by the DVR and UCAP system to negate the effect and retain a constant voltage V_L at the load end. The actual active and reactive power supplied by the series inverter can be computed using (3) from the rms values of injected voltage Vinj2a and load current I_{La} and ϕ is the phase difference between the two waveforms

$$P_{ref} = -\frac{2}{2} v_{sq}\, i_{qref}$$
$$Q_{ref} = -\frac{2}{2} v_{sq}\, i_{dref} \quad (4)$$

$$\begin{bmatrix} I_{refa} \\ I_{refb} \\ I_{refc} \end{bmatrix} = \begin{bmatrix} 1 & 0 \\ -\frac{1}{2} & \frac{\sqrt{3}}{2} \\ -\frac{1}{2} & -\frac{\sqrt{3}}{2} \end{bmatrix} \begin{bmatrix} cos\theta & sin\theta \\ -sin\theta & cos\theta \end{bmatrix} \begin{bmatrix} i_{dref} \\ i_{qref} \end{bmatrix} \quad (5)$$

The shunt inverter controller implementation is based on the id–iq method, which is modified to provide active and reactive power compensation, such that id controls there active power and iq controls the active power. Therefore, based on the references for active and reactive powers Pref and Qref, the reference currents iqref and idref in d–q domain can be calculated using(4), where vsq is the system voltage in q-domain and the reference currents are calculated using(5)

III. UCAP AND BIDIRECTIONAL DC–DC CONVERTER

A. *UCAP Bank Hardware Setup*

UCAPs can deliver very high power in a short time span they have higher power density and lower energy density when compared with Li-ion batteries [18], [19]. The major advantage UCAPs have over batteries is their power density characteristics, high number of charge–discharge cycles over their lifetime, and higher terminal voltage per module [5], [18]. These are ideal characteristics for providing active/reactive power support and intermittency smoothing to the distribution grid on a *short-term* basis. In [19], it is proposed that UCAPs are currently viable as short-term energy storage for bridging power in kilowatt range in the *seconds* to *few minutes* timescale. The choice of the number of UCAPs necessary for providing grid support depends on the amount of support needed, terminal voltage of the UCAP, dc-link voltage, and distribution grid voltages. For a 260-V dc-link voltage, it is practical and cost-effective to use three modules in the UCAP bank.

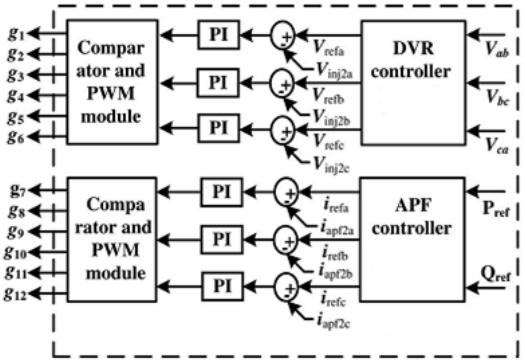

Fig. 3. Controller block diagram for DVR and APF.

Assuming that the UCAP bank can be discharged to 50% of its initial voltage (Vuc,ini) to final voltage (Vuc,fin) from 144V to 72V, which translates to depth of discharge of 75%, the energy in the UCAP bank available for discharge is given by

$$E_{UCAP} = \frac{1}{2} * C * \frac{(V_{uc,ini}^2 - V_{uc,fin}^2)}{60} \text{ W min} \quad (6)$$

$$E_{UCAP} = \frac{1}{2} * \frac{165}{2} * \frac{(144^2 - 72^2)}{60}$$
$$= 7128 \text{ W min}$$

B. *Bidirectional DC–DC Converter and Controller*

A bidirectional dc–dc converter is required as an interface between the UCAP and the dc-link, since the UCAP voltage varies with the amount of energy discharged, while the dc-link voltage has to be stiff.

The model of the bidirectional dc–dc converter and its controller are shown in Fig. 4(a). The dc–dc converter should operate in *Discharge* mode, while providing active/reactive power support and voltage sag compensation. The dc–dc converter should also be able to operate in bidirectional mode to be able to *charge* or absorb additional power from the grid during intermittency smoothing. In this paper, the bidirectional dc–dc converter acts as a boost converter, while *discharging* power from the UCAP and acts as a buck converter while *charging* the UCAP from the grid. Average current mode control, which is widely explored in literature [19], is used to regulate the output voltage of the bidi- rectional dc–dc converter in both *Buck* and *Boost* modes while *charging* and *discharging* the UCAP bank. This method tends to be more stable when compared with other methods like voltage mode control and peak current mode control. Average current mode controller is shown in Fig. 3, where the actual output voltage V_{out} is compared with the reference voltage V_{ref} and the error is passed through the voltage compensator
C1(s) that generates the average reference current Iucref.

C. Controller Implementation

Average current mode control is used to regulate the output voltage of the bidirectional dc–dc converter in both *Buck* and Boost modes, while charging and discharging the UCAP bank. While the UCAP-APF system is discharging power, the dc-link voltage Vout tends to be less than Vref, which causes the reference current Iucref to be positive, there by operating the dc–dc converter in Boost mode. Along similar lines, when the UCAP-APF system is absorbing power from the grid, the dc-link voltage Vout tends to be greater than Vref, which causes the reference current Iucref to be negative and the re by operating the dc–dc converter in Buck mode. Average current mode control technique is widely explored in the literature[19], and it was found as the ideal method for UCAP-APF integration as it tends to be more stable when compared with other methods like voltage mode control and peak current mode control. This is a major advantage in the present topology, where the stability of the dc–dc converter has to be ensured over a wide operating range and in both Buck and Boost modes of operation. Average current mode controller and the higher level integrated controller are shown in Fig.4, where the actual output voltage Vout is compared with the reference voltage Vref and the error is passed through the voltage compensator C1(s), which generates the average reference current Iucref. This is then compared with the actual UCAP current (which is also the inductor current) Iuc, and the error is then passed through the current compensator C2(s), The converter model for average current mode control is based on the following transfer functions developed in [19]

$$G_{id}(s) = \frac{V_{outv}\left(sC + \frac{2}{R}\right)}{s^2 LC + s\frac{L}{R} + (1-D)^2} \quad (7)$$

$$G_{vi}(s) = \frac{(1-D)\left[1 - \frac{sL}{R(1-D)^2}\right]}{\left(sC + \frac{2}{R}\right)} \quad (8)$$

The model of the dc–dc converter in average current mode control is shown in Fig.(5) that has two loops. The inner current loop Ti(s) has the current compensator C2(s), voltage modulator gain VM, and the transfer function Gid(s). The outer voltage loop Tv(s) constitutes the voltage compensator C1(s), current loop Ti(s), and the transfer function Gvi(s). The current compensator design C2(s) must be carried out initially and the voltage compensator C1(s) design is based on the design of the current compensator due to the dependency of C1(s) on C2(s). The current compensator C2(s) must be designed in such a way that at the cross over frequency of the current loop there is enough phase-margin to make the current loop Ti(s) stable and it should have a higher bandwidth when compared to the voltage loop Tv(s). Based on the criteria, the transfer functions of the current loop Ti(s) and the current compensator C2(s)are given by

$$T_i(s) = G_{id}(s) \cdot \frac{C_2(s)}{V_M}$$

$$C_2 = 1.67 + \frac{231.81}{s}$$

The closed-loop transfer function of the current loop is then given by

$$T_1(s) = \frac{T_i(s)}{1 + T_i(s)}$$

The voltage loop compensator $C_1(s)$ design is dependent on the PI compensator whose gain is adjusted to have the desired crossover frequency. Based on these criteria, the transfer functions of the voltage loop $T_V(s)$. and compensator $C_1(s)$ is given by

$$T_v(s) = G_{vi}(s) C_1(s) T_1(s)$$

$$C_1(s) = 3.15 + \frac{1000}{s}$$

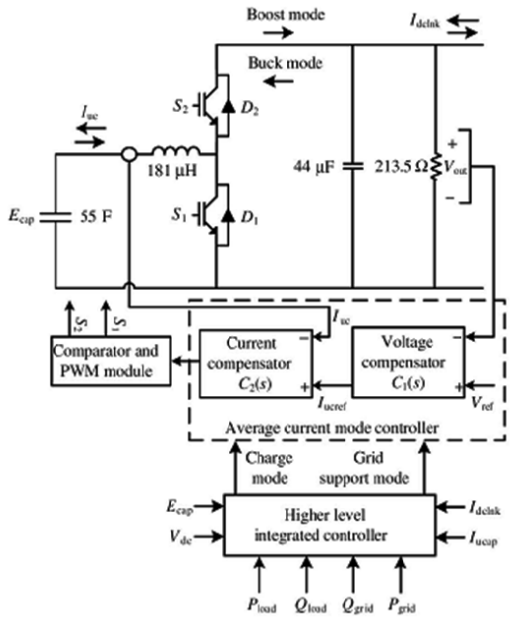

Figure 4 Model of Bi-directional dc-dc converter and its controller

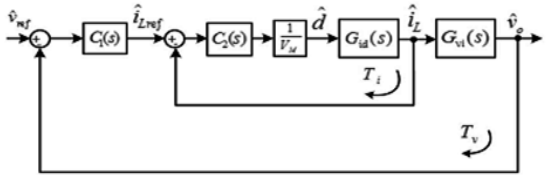

Figure 5 Model of the dc-dc converter in average current mode

The transfer function of the plant $G_{Vi}(s)$ along with the transfer function of $C_1(s)$ of the voltage compensator and the overall voltage loop transfer function Tv(s) are shown in Figure (5). It can be observed that the voltage loop Tv(s) has a crossover frequency of around 150 Hz with a phase margin of 73^0, which provides a stable dynamic response. The stability and dynamic performance of the voltage loop Tv(s) determine the stability and dynamic response of the overall system.

D. Higher level intergrated controller

The higher level integrated controller is designed to make system level decisions on the inverter and dc–dc converter controllers. Based on various system parameters like R_{load}, Q_{load}, P_{grid}, Q_{grid}, V_{UCAP}, V_{dc}, $I_{dc\ link}$, and $I_{u\ cap}$, the higher level integrated controller will decide on operating in one of the following modes active power support mode, reactive power support mode, renewable intermittency smoothing mode, sag/swell compensation mode, and UCAP charge mode.

In active power support mode and renewable intermittency smoothing mode, the UCAP-PC system must provide active power to the grid. Therefore, the active power capability of the UCAP-PC system must be assessed by the higher level integrated controller. Based on the P_{grid}, and R_{load} values, the reference P_{ref} is calculated in the higher level integrated controller, and it will decide if the UCAP has enough energy to respond to the P_{ref} command based on the UCAP state of charge. If the UCAP has enough capacity to respond to the request, then the dc–dc converter controller is operated in grid support mode otherwise, it is operated in charging mode, where the UCAP is recharged and the power request is met at a later time. In grid support mode, the dc–dc converter will operate in a bidirectional fashion in both Buck and Boost modes to respond to the active power requests and regulate the dc-link voltage in a stable fashion, while the inverter controller should respond such that the Commanded Pref is supplied by the inverter through current control.

In reactive power support mode ,the UCAP-PC system must provide reactive power to the grid. In this mode, the UCAP-PC does not provide any active power to the grid and even the PC losses are supplied by the grid. Based on the Q_{grid}, and Q_{load} values the reference Q_{ref}, is calculated in the higher level integrated controller. In this mode, the dc–dc converter controller can be programmed to operate in grid support mode directly because the active power requirement for operating in this mode is minimal. Therefore, the goal of the dc–dc converter controller is to regulate the dc-link voltage in a stable fashion, while the inverter controller should respond such that the commanded Q_{ref}, is supplied by the inverter through current control.

In sag/swell compensation mode, the UCAP-PC system is programmed to prevent sensitive loads from disturbances on the supply-side like voltage sag or voltage swell. These disturbances require short-term energy storage, and in this mode, the dc–dc converter controller can be programmed to operate in grid support mode. Therefore, the goal of the dc–dc converter controller is to regulate the dc-link voltage in a stable fashion during both sag/swell events. It is also required that the dc–dc converter

be able to discharge and meet the active power requirements during a voltage sag and to be able absorb active power in a stable fashion during a voltage swell event.

In charge mode, the UCAP is recharged by absorbing active power from the grid when the UCAP state of charge falls below 50%. The rate at which the UCAP can be charged is assessed by the higher level integrated controller based on the P_{grid} and P_{load} values and the reference P_{grid}, P_{ref} is calculated. Then the dc–dc converter controller is commanded to operate in charge mode, wherein the dc–dc converter will operate in Buck Mode to absorb the power from the grid and the inverter controller must respond to supply commanded Pref.

IV. SIMULATION RESULTS

The simulation of the proposed UCAP integrated power conditioner system is carried out in MATLAB environment. The system response for a three-phase voltage sag which lasts for 0.1s and has a depth of 0.64p.u. is shown in Fig.6.1–6.5. It can be observed from Fig.6.1 that during voltage sag, the source voltage V_{srms}, is reduced to 0.36p.u., while the load voltage V_{Lrms} is maintained constant at around 1.01p.u. due to voltages injected in-phase by the series inverter. This can also be observed from the plots of the line–line source voltages (V_{sab}, V_{sbc} and V_{sca}) [Fig.6.2], the line–line load voltages (V_{Lab}, V_{Lbc} and V_{Lca}) Fig.6.3 the plots of the bidirectional dc-dc converter are presented, and it can be observed that the dc-link voltage Vfdc is regulated at 260V, the average dc-link current Idclnkav and the average UCAP current Iucav increase to provide the active power required by the load during the sag. This can also be observed from various active power plots shown in Fig.6.2, where the power supplied to the load Pload remains constant even during the voltage sag when the grid power V_{grid} is decreasing. The active power deficit of the grid is met by the DVR power P_{dvr}, which is almost equal to the input power to the inverter P_{dc} in available from the UCAP. Therefore, it can be concluded from the plots that the active power deficit between the grid and load during the voltage sag event is being met by the UCAP-based energy storage system through bidirectional dc–dc converter and the inverter. It can also be noticed that the grid reactive power Q_{grid} reduces during the voltage sag while Q_{dvr} increases to compensate for the reactive power loss in the system. Similar analysis canal so be carried out for voltage.

The proposed UCAP integrated power conditioner system's performance is then simulated for the active and reactive power

support case. The system response is simulated for the reactive power support mode for the initial 0.225 s, where i_{dref}=−15 A for the initial 0.225 s, which translates to a Q_{ref} of 3819 Var from eq(6.4). For the rest of the 0.225 s, the system response is simulated for active power support mode with $i_{r\,ref}$=−12A, which translates to Pref of 3054 W. While the UCAP current and the corresponding dc-link current are higher for active power support case when compared with the reactive power support case. In figure. 6.6 and figure. 6.7, the active and reactive power curves for both the modes are presented, and it can be observed from the active and reactive power curves that the reactive power Qapf reaches the commanded value in the reactive power support mode and the active power is supplied by the UCAP is minimal in this case. It can be observed that during the voltage sag, Ecap is decreasing rapidly and Iucav is increasing rapidly while Vfdc and Idclnkav are constant

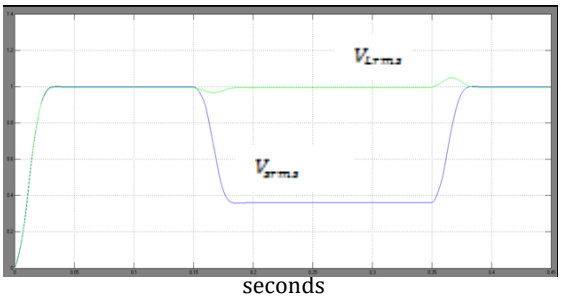

Figure 6.1. Source and load rms voltages Vsrms and VLrms during sag

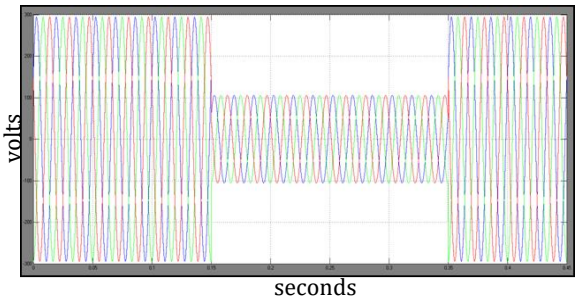

Figure 6.2. Source voltages Vsab (blue), Vsbc (red), and Vsca (green) during sag

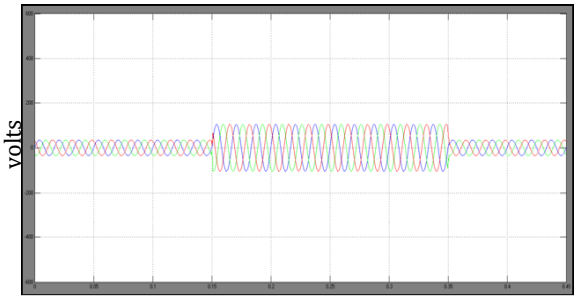

Figure 6.3. Injected voltages Vinj2a (blue), Vinj2b (red), and Vinj2c (green) during sag

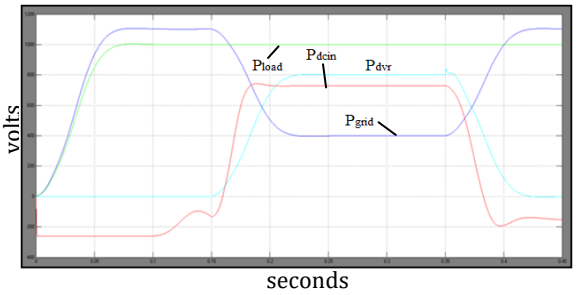

Figure 6.4. Active power of grid, load and inverter during voltage sag

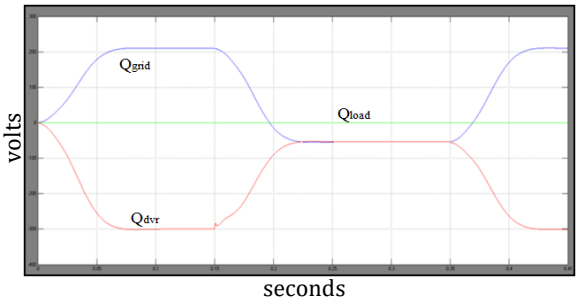

Figure 6.5. Reactive power of grid, load inverter during voltage sag

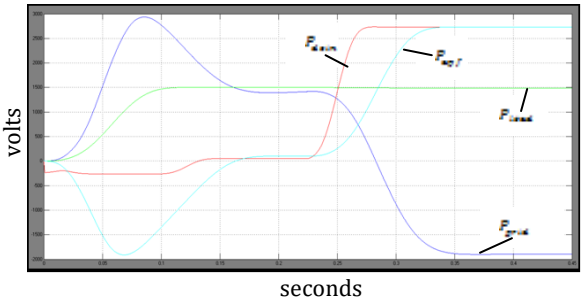

Figure 6.6. Reactive powers of grid, load and converters

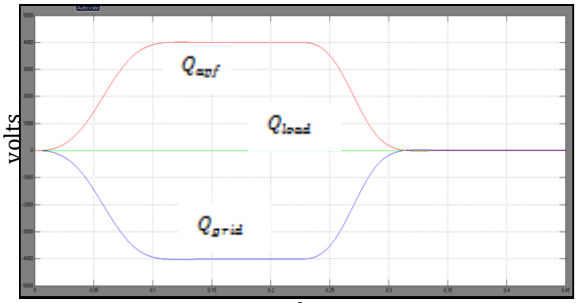

Figure 6.7. Reactive powers of grid, load and converters

Therefore, the dc–dc converter is able to regulate the dc-link voltage to 260 V and operate in Boostmode to discharge active power during a voltage sag event to meet the active power deficit between the grid and the load. In versions of the line–neutral injected voltage Vinj line–line source voltage VLab the line–line load voltage VLab, and the load current ILa during the voltage sag event. It can be observed that during the voltage sag event the magnitude of Vsab is reduced while the magnitude of VLabre mains constant due to the injected voltage Vinj which increases during the voltage sag event to compensate for the voltage sag. Therefore, from both inverter and dc–dc converter experimental waveforms, it can be concluded that the UCAP integrated DVR system hardware setup is able to respond instantaneously to compensate voltage sags.In the active power support mode, the UCAP and the inverter system supply the required active power and the additional power flows back into the grid. This can be observed from the P_{dcin}, P_{grid}, P_{load}, and P_{apf} waveforms.

CONCLUSION

This paper presents the concept of integrating UCAP-based rechargeable energy storage to a power conditioner system to improve the power quality of the distribution grid. With this integration, the DVR portion of the power conditioner will be able to independently compensate voltage sags and swells and the Active Power Filter (APF) portion of the power conditioner will be able to provide active/reactive power support and renewable intermittency smoothing to the distribution grid. UCAP integration through a bidirectional dc–dc converter at the dc-link of the power conditioner is perfoemed. The control strategy of the series inverter (DVR) is based on inphase compensation and the control strategy of the shunt inverter (APF) is based on $id - iq$ method. Designs of major components in the power stage of the bidirectional dc–dc converter are discussed. Average current mode control is used to regulate the output voltage

of the dc–dc converter due to its inherently stable characteristic. A higher level integrated controller that takes decisions based on the system parameters provides inputs to the inverters and dc–dc converter controllers to carry out their control actions. The simulation of the integrated UCAP-PC system which consists of the UCAP, bidirectional dc–dc converter, and the series and shunt inverters is carried out using MATLAB. The simulation of the UCAP-PC system is carried out using MATLAB. Results from simulation and experiment agree well with each other thereby verifying the concepts introduced in this paper. Similar UCAP based energy storages can be deployed in the future in a microgrid or a low-voltage distribution grid to respond to dynamic changes in the voltage profiles and power profiles on the distribution grid.

REFERENCES

[1] N. H. Woodley, L. Morgan, and A. Sundaram, "Experience with an inverter-based dynamic voltage restorer," IEEE Trans. Power Del., vol. 14, no. 3, pp. 1181–1186, Jul. 1999.

[2] J. G. Nielsen, M. Newman, H. Nielsen, and F. Blaabjerg, "Control and testing of a dynamic voltage restorer (DVR) at medium voltage level," IEEE Trans. Power Electron., vol. 19, no. 3, pp. 806–813, May 2004.

[3] V. Soares, P. Verdelho, and G. D. Marques, "An instantaneous active and reactive current component method for active filters,"IEEE Trans. Power Electron., vol. 15, no. 4, pp. 660–669, Jul. 2000.

[4] H. Akagi, E. H. Watanabe, and M. Aredes, Instantaneous Reactive Power Theory and Applications to Power Conditioning, 1st ed. Hoboken, NJ, USA: Wiley/IEEE Press, 2007.

[5] K. Sahay and B. Dwivedi, "Supercapacitors energy storage system for power quality improvement: An overview,"J. Energy Sources, vol. 10, no. 10, pp. 1–8, 2009.

[6] B. M. Han and B. Bae, "Unified power quality conditioner with super-capacitor for energy storage," Eur. Trans. Elect. Power, vol. 18, pp. 327–343, Apr. 2007.

[7] P. F. Ribeiro, B. K. Johnson, M. L. Crow, A. Arsoy, and Y. Liu, "Energy storage systems for advanced power applications,"Proc. IEEE, vol. 89, no. 12, pp. 1744–1756, Dec. 2001.

[8] A. B. Arsoy, Y. Liu, P. F. Ribeiro, and F. Wang, "StatCom-SMES,"IEEE Ind. Appl. Mag., vol. 9, no. 2, pp. 21–28, Mar. 2003.

[9] J. Rittershausen and M. McDonagh,Moving Energy Storage from Concept to Reality: Southern California Edison's Approach to Evaluating Energy Storage [Online]. Available: www.edison.com/content/ dam/ eix/ documents/innovation/smart-grids/Energy-Storage-Concept-toReality-Edison.pdf, accessed on 15 Jul., 2014.

[10] M. Branda, H. Johal, and L. Ion, "Energy storage for LV grid support in Australia," in Proc. IEEE Innov. Smart Grid Tech. Asia (ISGT), Nov. 13–16, 2011, pp. 1–8.

[11] W. Li, G. Joos, and J. Belanger, "Real-time simulation of a wind turbine generator coupled with a battery supercapacitor energy storage system," IEEE Trans. Ind. Electron., vol. 57, no. 4, pp. 1137–1145, Apr. 2010.

[12] P. Thounthong, A. Luksanasakul, P. Koseeyaporn, and B. Davat, "Intelligent model-based control of a standalone photovoltaic/fuel cell power plant with supercapacitor energy storage,"IEEE Trans. Sustain. Energy, vol. 4, no. 1, pp. 240–249, Jan. 2013.

[13] X. Li, D. Hui, and X. Lai, "Battery energy storage station (BESS)-based smoothing control of photovoltaic (PV) and wind power generation fluctuations,"IEEE Trans. Sustain. Energy, vol. 4, no. 2, pp. 464–473, Apr. 2013.

[14] J. Tant, F. Geth, D. Six, P. Tant, and J. Driesen, "Multiobjective battery storage to improve PV integration in residential distribution grids,"IEEE Trans. Sustain. Energy, vol. 4, no. 1, pp. 182–191, Jan. 2013.

[15] Y. Ru, J. Kleissl, and S. Martinez, "Storage size determination for gridconnected photovoltaic systems,"IEEE Trans. Sustain. Energy,vol.4, no. 1, pp. 68–81, Jan. 2013

[16] S. Teleke, M. E. Baran, S. Bhattacharya, and A. Q. Huang, "Rule-based control of battery energy storage for dispatching intermittent renewable sources," IEEE Trans. Sustain. Energy, vol. 1, no. 3, pp. 117–124, Oct. 2010.

[17] T. K. A. Brekkenet al., "Optimal energy storage sizing and control for wind power applications,"IEEE Trans. Sustain. Energy, vol. 2, no. 1, pp. 69–77, Jan. 2011.

[18] S. Santoso, M. F. McGranaghan, R. C. Dugan, and H. W. Beaty,Electrical Power Systems Quality, 3rd ed. New York, NY, USA: McGraw-Hill, Jan. 2012.

[19] R. W. Erickson and D. Maksimovic,Fundamentals of Power Electronics, 2nd ed. Norwell, MA, USA: Kluwer, 2001